

The Dynamics of Hurricane Balls

W. L. Andersen*

Department of Physical Sciences, Eastern New Mexico University, Portales, NM 88130

Steven Werner†

Engineering Dept, Lear Jet, Wichita, KS 67209

(Dated: June 11, 2015)

Abstract

We examine the theory of the Hurricane Balls toy. This toy consists of two steel balls, welded together that are sent spinning on a horizontal surface somewhat like a top. Unlike a top, at high frequency the symmetry axis approaches a limiting inclination that is not perpendicular to the surface. We calculate (and experimentally verify) the limiting inclinations for three toy geometries. We find that at high frequencies, Hurricane Balls provide an easily realized and testable example of the Poincaré theory of freely rotating symmetrical bodies.

I. INTRODUCTION

Recently an interesting physics toy under the name Hurricane Balls was introduced to the marketplace.¹ This toy consists of two identical ball bearings joined together in a manner similar to figure 1. After setting the apparatus spinning on one of the balls by hand, a plastic pipe is used to blow at one side to increase the angular velocity. Unlike a coin, the Hurricane Balls apparatus does not spin fully upright at high frequencies. The physics of this toy is an instructive exercise in the theory of rigid body motion. The toy moves primarily under the influence of gravity and rolling friction. As discussed below in more detail, the rolling friction enforces a constraint which sets the frequency of rotation of the toy about the symmetry axis equal to the rotational frequency of the symmetry axis about the direction of gravity. Remarkably, this constraint prevents the toy from becoming vertical at high frequencies. The main conclusion of this paper is that at sufficiently high frequencies, the external torque on the toy becomes negligible in determining its motion so that Poincaré's theory of a freely rotating body becomes applicable in the determination of the limiting inclination of the toy.



FIG. 1. Custom made Hurricane Balls and thermal paper affixed to vertical metal plate. Commercially available Hurricane Balls are welded together rather than being connected by a shaft. The line across the bottom is a reference line created one ball radius off the surface by dragging the balls across the plate. The strike marks come from slowly moving the plates up to the whirling balls until the upper ball strikes the paper.

II. TREATMENT INCLUDING GRAVITY

Before proceeding to the application of Poincaré's free body solution, we examine the motion including external torque. We shall consider only gravity and the force exerted by the horizontal surface. Dissipative forces such as drag and the Magnus effect will be ignored. Our analysis is similar to the treatment of coin whirling in reference 2. In particular, we consider motion in which the center of mass remains at rest while the toy rolls and spins without slipping. We take each ball to have mass M and radius R . We choose the origin to be the stationary center of mass at the point of contact of the two balls. The torque is then due to the normal force of the surface. Assuming that the toy is supported by the surface, the normal force is $2Mg$. The equation of motion of the toy is

$$\boldsymbol{\tau} = \frac{d\mathbf{L}}{dt} \quad (1)$$

Referring to Fig. 2 to define the angle θ used to describe the inclination of the toy, we see that the torque magnitude is $\tau = 2Mg OA = 2MgR \sin \theta$.

We can also use figure 2 to understand the consequence of the non-slip rolling constraint. Two angular velocities will be crucial in understanding the motion. The angular velocity of the toy about its symmetry axis is ω_3 . The symmetry axis itself rotates about an axis parallel to gravity and passing through the centre of mass of the toy. The angular velocity of the symmetry axis about the direction of gravity is called Ω . The total angular velocity of the toy is

$$\boldsymbol{\omega} = \boldsymbol{\Omega} + \boldsymbol{\omega}_3 \quad (2)$$

The lower ball traces a circle on the ground centred on the point where the vertical axis $\boldsymbol{\Omega}$ passing through the centre of mass intersects the ground at O . The diameter of this circle is $AB = 2R \sin \theta$. The locus of points of the lower ball which successively contact the ground to trace this circle themselves form a circle on the ball, shown in profile (figure 2) with antipodal points A and A' . This circle is the intersection of a conical surface with its apex at the ball's centre and aperture 2θ . The diameter of this circle is $A'A = 2R \sin \theta$. Since $A'A = AB$, the circumferences of these circles are equal and the no-slip condition implies $\Omega = \omega_3$. This constraint is the essential difference between a standard top and Hurricane Balls.

The validity of the no-slip assumption is tested in the video available as an online supplement to this paper. A stroboscope is used to freeze the motion of a whirling Hurricane Balls toy, thus providing a measure of Ω . A piece of red tape affixed to the upper ball reveals the angular position of the balls about axis 3. Combined with the strobe illumination, this provides a measure of $\Omega - \omega_3$. If $\Omega = \omega_3$ we expect the tape to appear stationary when the strobe illumination freezes the balls' motion. In fact the tape moves, but only very slowly in comparison with the rotational frequency of the toy (about 40 – 50 Hz). We find that Ω differs from ω_3 by only a hertz or less. At least part of the slight failure of the no-slip assumption is likely due to the necessity of corralling the Hurricane Balls on a spherical surface to prevent translational drifting. Two surfaces of different curvature are tried. The smaller radius of curvature results in a greater difference between Ω and ω_3 . This can be understood by visualizing Fig. 2 with a spherical supporting surface. Under that geometry the aperture of the cone discussed above does not quite equal 2θ . Air resistance and the Magnus force might also contribute to the slight slipping. Regardless of such complications, however, the no-slip assumption is seen to be a good approximation.

In addition to the symmetry axis, we adopt body fixed axes 1 and 2 such that 1 – 2 – 3 define a right-handed coordinate system at the centre of mass. In Figure 2, axis 2 is instantaneously directed toward the reader while 1 lies in the page perpendicular to 2 and 3. These are principal axes.

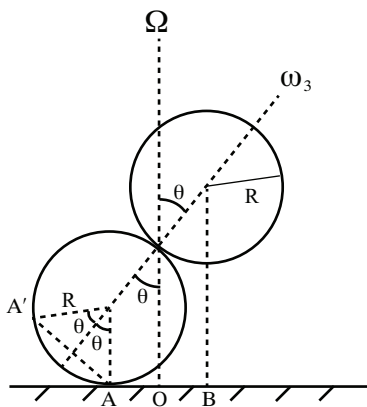


FIG. 2. The toy in instantaneous profile: the sense of ω_3 depends on the sense of Ω , the angular velocity of the symmetry axis about the direction of gravity.

The angular momentum of the toy is $\mathbf{L} = \mathbf{I} \cdot \boldsymbol{\omega}$ where \mathbf{I} is the rotational inertia tensor.

In our body fixed system, \mathbf{I} is represented by

$$\mathbf{I} = MR^2 \begin{pmatrix} \frac{14}{5} & 0 & 0 \\ 0 & \frac{14}{5} & 0 \\ 0 & 0 & \frac{4}{5} \end{pmatrix} \quad (3)$$

It is useful to express $\boldsymbol{\Omega}$ as the sum of projections along the principal axes. Using the geometry of Fig. 3 we write

$$\boldsymbol{\Omega} = \boldsymbol{\Omega}_\perp + \boldsymbol{\Omega}_3 \quad (4)$$

where $\Omega_\perp = \Omega \sin \theta$ and $\Omega_3 = \Omega \cos \theta$. The total angular momentum then has the three contributions $\mathbf{I} \cdot (\boldsymbol{\Omega} + \boldsymbol{\omega}_3) = \mathbf{I} \cdot (\boldsymbol{\Omega}_\perp + \boldsymbol{\Omega}_3 + \boldsymbol{\omega}_3)$.

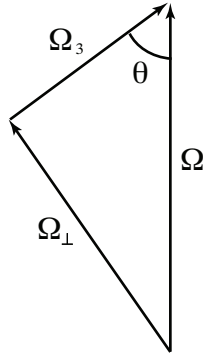


FIG. 3. The angular velocity Ω is projected onto principal directions.

Fig. 4 depicts these three contributions to the angular momentum including the constraint $\boldsymbol{\omega}_3 = \boldsymbol{\Omega}$. The angular momentum lies in the plane of Fig. 4. Also shown are the horizontal components of these three contributions. The total horizontal angular momentum has magnitude

$$L_\parallel = I_3 \Omega \sin \theta + I_3 \Omega \cos \theta \sin \theta - I_1 \Omega \sin \theta \cos \theta \quad (5)$$

The torque is always instantaneously perpendicular to the plane of Fig. 4 so the rate of change of angular momentum has the geometry shown in Fig. 5

We see that the motion of the total angular momentum vector defines an inverted cone with base of radius L_\parallel . The vector \mathbf{L}_\parallel traces this circle with angular frequency Ω . The right hand side of Eqn. 1 then has the magnitude

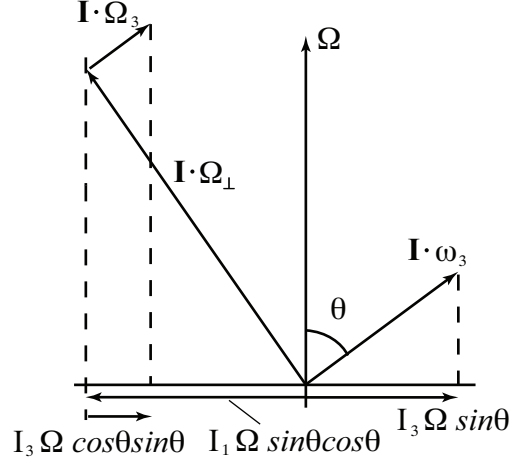


FIG. 4. Angular velocities and angular momenta. The constraint $\omega_3 = \Omega$ has been imposed in calculating the horizontal components.

$$\left| \frac{d\mathbf{L}}{dt} \right| = \Omega L_{\parallel} \quad (6)$$

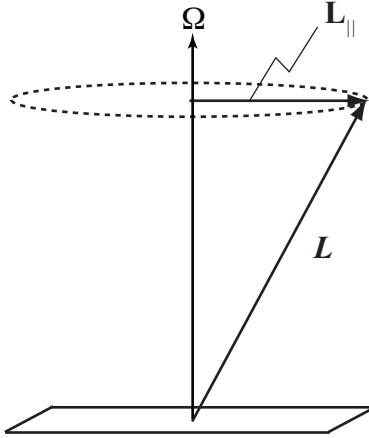


FIG. 5. The rate of change of angular momentum is ΩL_{\parallel} .

Using $\tau = 2MgR \sin \theta$ and Eqn. 5 we see that Eqn. 1 implies

$$\Omega(I_3 \Omega \sin \theta + I_3 \Omega \cos \theta \sin \theta - I_1 \Omega \sin \theta \cos \theta) = 2MgR \sin \theta \quad (7)$$

Substituting for the rotational inertia components we get

$$\frac{2}{5} - \cos \theta = \frac{g}{R\Omega^2} \quad (8)$$

From a mathematical point of view, Eqn. 8 indicates that a sufficiently large rotational velocity ensures that the limiting angle is identical to that of free body motion ($g = 0$) subject to the constraint $\Omega = \omega_3$. Whether the constraint is enforced by rolling friction or some other means is irrelevant.

From a physical point of view, we see that at high frequencies the angular momentum is nearly vertical with a comparatively small horizontal component which precesses in response to the external torque. For $R\Omega^2 \gg g$, the horizontal component of angular momentum becomes negligible compared to the total angular momentum. At the angle defined by Eqn. 8 the expression for L_{\parallel} , Eqn. 5, vanishes in the limit $g/R\Omega^2 \rightarrow 0$. Thus, $\dot{\mathbf{L}} \rightarrow 0$ and the motion is practically indistinguishable from free body motion.

III. POINSON'S THEORY

Poinsot's treatment is based on Euler's equations of motion

$$I_1\dot{\omega}_1 + (I_3 - I_2)\omega_3\omega_2 = 0; \quad (9)$$

$$I_2\dot{\omega}_2 + (I_1 - I_3)\omega_1\omega_3 = 0; \quad (10)$$

$$I_3\dot{\omega}_3 = 0 \quad (11)$$

Poinsot's solution yields the geometric result shown in Fig. 6. The cone centred on ω_3 (traditionally the body cone) rolls without slipping on the cone centred on \mathbf{L} (the space cone). The line of intersection is the total angular velocity vector of the toy. The angle of inclination is $\theta = \alpha_s + \alpha_b$.

If we define the oblateness $\beta = (I_3 - I_1)/I_1$ then it can be shown that the angular velocity ω rotates about the 3-body axis at the angular frequency $\beta\omega_3$.

It can be further shown³ that the space and body cones are related by

$$\cos \alpha_s = \frac{1 + \beta \cos^2 \alpha_b}{\sqrt{1 + (2\beta + \beta^2) \cos^2 \alpha_b}}. \quad (12)$$

The frictional rolling constraint $\Omega = \omega_3$ amounts to the requirement $\alpha_s = \alpha_b$. Setting $\alpha \equiv \alpha_s = \alpha_b$ in Eq. (12) determines the cosine to be

$$\cos \alpha = \sqrt{\frac{7}{10}}. \quad (13)$$

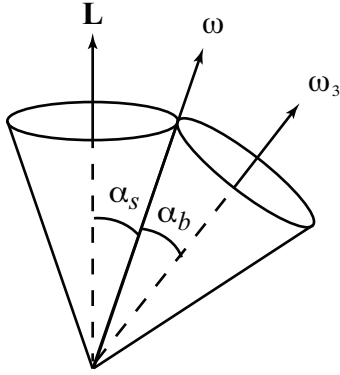


FIG. 6. The Poincaré construction. The body cone (centred on ω_3) rolls without slipping on the space cone (centred on \mathbf{L}).

Considering that $\theta = 2\alpha$ this result agrees with Eq. (8) for $R\Omega^2 \gg g$.

IV. EXPERIMENTAL

The inclination angle θ was measured for three different geometries of custom manufactured Hurricane Balls:

- two solid balls ($R = 0.720$ cm) touching
- two solid balls ($R = 0.794$ cm) connected by a rod of length $L = 1.21$ cm. This set of Hurricane Balls is shown in Fig. 1.
- two hollow balls touching, interior and exterior radii of 1.60, 1.91 cm

The generalization of Eqn. 8 to an arbitrary axially symmetric body in the limit $g/R\Omega^2 \rightarrow 0$ is

$$\cos \theta = \frac{I_3}{I_1 - I_3} \quad (14)$$

Balls in contact were silver soldered with a Bernzomatic MAPP torch after a small spot was scuffed on the surface of each sphere. Ball bearings were threaded and joined by a threaded shaft for the second case.

We measured the Hurricane Ball angles with a machined right angle strike plate. The plate surface was affixed with thermal paper that produced a mark when contacted by the

balls. Fig. 1 illustrates the technique. Strike marks and a reference line one ball radius above the surface are visible. The distance between the reference line and a strike mark, h , is related to the centre to centre distance D and angle θ by

$$h = D \cos \theta \quad (15)$$

To determine the centre to centre distance, we measured the overall length of the balls and subtracted the measured diameter. The soldered balls were slightly shorter than two times the diameter since flat spots were ground on the ball surfaces to help make a good silver solder connection. Ten strike marks were produced and measured for each toy geometry to calculate an average and standard deviation for θ .

Predicted and measured θ are shown in table I. Agreement of theory and experiment seems satisfactory; though, there is some issue with the hollow balls. This could be due to a manufacturing anomaly. Each hollow sphere is made of two hemispheres welded together. The thickness might not be uniform due to the weld. Sticking a tooth pick probe in the hole drilled to accept the rod revealed overfill from the weld. If we suppose that overfill of mass m increases both I_1 and I_3 by mR^2 , then according to Eqn. 14 $\cos \theta$ is increased by $m/2M$. Given the approximate mass $2M = 170$ g for the hollow ball assembly, we see that a 4 g overfill would account for the discrepancy between theory and experiment. An alternative explanation, error in R_1 or R_2 , seems less likely. We find that a measurement error of about 0.2 cm would be necessary to reconcile theory and experiment.

TABLE I. Limiting inclination at high frequency for three geometries. The two radii indicated for the shell are the inner and outer radii.

ball type	$R(\text{cm})$	$L(\text{cm})$	θ_{theory}	θ_{exp}
solid	0.720	0	66.4	65.5 ± 0.8
solid	0.794	1.21	76.9	75.8 ± 0.4
shell	1.60, 1.91	0	55.2	53.4 ± 0.6

V. CONCLUSION

At high frequencies, Hurricane Balls provide an easily realized example of the Poincot theory of freely rotating symmetrical bodies. The rolling constraint couples precession and symmetry axis rotation to produce a limiting inclination that can be measured to test Poincot's theory of free body motion.

* William.Andersen@mailaps.org; permanent address: Station 33, Eastern New Mexico University, Portales, NM 88130

† steve.werner@cox.net

¹ available at <<http://www.grand-illusions.com>>; demonstration video at <<http://www.youtube.com/watch?v=cvq81aPb498>>.

² W. L. Andersen, "Noncalculus Treatment of Steady-State Rolling of a Thin Disk on a Horizontal Surface," *Phys. Teach.* **45** (7), 430–433.

³ Keith R. Symon, *Mechanics*, 3rd edition (Addison-Wesley, Reading, 1971), 444–451.